Kinetic Interpretation of Influence of Sodium Chloride Concentration and Temperature on Xanthan Gum Dispersion Flow Model

M. DOLZ, M. J. HERNÁNDEZ, J. DELEGIDO

Department of Thermodynamics, University of Valencia, 46100 Burjassot, Valencia, Spain

Received 31 July 2000; accepted 27 March 2001

ABSTRACT: The present study derives a fixed-concentration (0.4%) xanthan gum dispersion flow model for different molar concentrations of sodium chloride (0–0.25*M*) and different temperatures (20–70°C). The Ostwald–de Waele model is used in all cases. A temperature rise reduces the shear-thinning characteristics of the systems, although the power law index is much less sensitive to changes in temperature when NaCl is added, even in very small amounts. The lowest consistency values correspond to the dispersions formulated in the absence of salt, the highest values are observed for molar values of ≥0.15, and there are decreases in consistency upon raising the temperature in all cases. The viscous behavior of the dispersions is interpreted using the Eyring equation. The activation energy and the free volume decrease when the shear rate is increased. The addition of NaCl, regardless of the molar concentration involved, provokes an important decrease of the activation energy. The free volume is independent of the molar concentration of NaCl for molar values >0.025. These results are related to the structure of the dispersions. © 2002 John Wiley & Sons, Inc. J Appl Polym Sci 83: 332–339, 2002

Key words: xanthan gum; viscosity; temperature; sodium chloride concentration; Eyring equation

INTRODUCTION

Xanthan gum is a polymer that is industrially obtained from the bacterium *Xanthomonas campestris*. In the 1960s it was studied in detail, and its use is authorized in the food industry. Many of the applications of xanthan gum are a consequence of its rheological behavior.[1–5] Under resting conditions, the long xanthan molecules combine to form a 3-dimensional network. On applying energy to the system, these weak bonds disrupt and the viscosity of the preparation decreases. The drop in viscosity observed at high shear rates improves the mixing and flow properties while the high viscosity seen at low shear rates and at rest contributes to the stabilization of foam, emulsions, and suspensions.[6]

In foodstuff applications xanthan gum is used in salad dressings, creams, sauces, syrups, desserts, beverages, and prepared and frozen foods. In the cosmetics and pharmaceutical industry it is used in lotions, creams, cough syrups, and toothpaste. In the industrial setting it is employed in oils, hydraulic fluid, pesticides, animal fodder, cleaning products, dyes, and metal bathing.[6] The most usual concentrations employed are 0.1–0.5% in beverages, soups, and sauces[5] and 0.7–1.0% in toothpaste.[7]

Due to its multiple applications in the food industry, studies were conducted on the effects of the addition of salts on the rheological behavior of

Correspondence to: M. Dolz (manuel.dolz@uv.es).

Journal of Applied Polymer Science, Vol. 83, 332–339 (2002)

xanthan,[8] as well as the results of mixing xanthan with other polymers.[7,9–11] In general, the effects of the addition of salt depend on the xanthan concentration.[1] At concentrations of under 0.15–0.40%, the addition of salt reduces the viscosity of the preparation; however, at higher xanthan concentrations salt is seen to increase the viscosity of the formulation.[12] The addition of salt to xanthan modifies the ionic charge of the medium. In 1992 Clark interpreted these effects assuming that in dilute xanthan solutions in the absence of salt the xanthan ionic charges are not neutralized, thus leading to an expansion of the molecules and the generation of a semirigid structure with an increased hydrodynamic volume.[8] However, when salt is added, the ionic charges are neutralized and the molecules decrease in volume, adopting a coil shape.[4] In solutions with higher xanthan concentrations (above approximately 0.3%) the effect of the intermolecular bonds in terms of rheological behavior, consistency, and plasticity is enhanced by the increased ionic activity; this effect is comparatively more important than the result of reducing the size of the molecules. As a result, the addition of salt at high concentrations increases the viscosity of the preparation.

The study of the effects of temperature on the rheological behavior of xanthan is essential for its many applications in both industry formulations. In this sense, at low shear rates the viscosity of xanthan is known to decrease[13,14] when the temperature rises from 20 to 70°C. However, the presence of small amounts of salt (0.1–0.15%) in the xanthan formulations leads to increased thermal stability with only slight variations in the viscosity upon modifying the temperature. This property is used in creams and sauces[6] to secure constant viscosity values at temperatures around 80°C.

In general, the study of variations in fluid viscosity with temperature is made on an empirical basis. However, Eyring developed an approximation based on the kinetic theory of fluid that makes it possible to estimate the viscosity from other physical parameters[4,15,16] or to account for the possible structural configuration of a fluid once its viscous behavior is known as was attempted in the present study.

According to this theory, the fluid molecules are in constant motion; however, as a consequence of the compact packing of the molecules, movement is limited to vibration within the confines of the neighboring molecules. These confines are represented by a potential energy barrier ($\Delta G_o^{\ddagger}$) for each molecule. According to Eyring, a fluid at rest undergoes continuous rearrangements whereby a molecule can escape from its confinement toward a contiguous gap; as a result, the flow capacity of the system must be related to the number of possible gaps and to the corresponding free activation energy for flow ($\Delta G_o^{\ddagger}$). If the fluid is subjected to shear stress (σ), the potential energy barrier is distorted; if the sense of the applied stress coincides with the fluid movement, then a decrease in activation energy results with respect to the value at rest:

$$\Delta G^{+} = \Delta G_o^{+} - \Delta G(\sigma) \tag{1}$$

Based on these considerations and according to Eyring, the viscosity (η) of a given fluid obeys an equation of the following type:

$$\eta = A \exp(\Delta G_o^{+}/RT) \tag{2}$$

where A is a coefficient that depends on the free volume of the fluid studied, which has the form $A = f(1/[V - V_s])$, where V represents the molar volume of the fluid at the temperature (T) and pressure of the experiment and V_s is the molar volume following compression to reduce the free volume (V_L) to zero.[16] Thus, the free volume can be expressed as

$$V_L = V - V_s = C/A \tag{3}$$

where C is a constant for each fluid. Equation (2) is adequate for describing the variation of the viscosity with temperature[2,4,14,17] (except for large fluctuations of the latter).

If appreciable density (ρ) changes occur with the temperature T, then eq. (2) can be expressed as follows using the concept of cinematic viscosity:

$$\nu = \eta/\rho = A' \exp(E/RT) \tag{4}$$

However, studies of this kind usually employ empirical equations, the validness of which applies to larger temperature intervals or the non-Newtonian nature of the fluid is taken into consideration.[18] In this context, Vogel proposed the following very simple equation that is valid for Newtonian fluids over a broad temperature range:

$$\eta = A \exp\left(\frac{B}{T - T_o}\right) \quad (5)$$

where A, B, and T_o are constants for each fluid. The equation proposed by Vogel can be corrected for non-Newtonian fluids that satisfy the power law as follows:

$$\eta = K\dot{\gamma}^{n-1}\exp[-\alpha(T - T_o)] \quad (6)$$

or alternatively

$$\ln \eta = A_0 + (n - 1)\ln \dot{\gamma} - \alpha T \quad (7)$$

However, in some systems the exponential dependency of the viscosity on the temperature is not very precise. In such cases, Kennedy[19] proposed the following second-order model with respect to the shear rates ($\dot{\gamma}$) and T:

$$\ln \eta = A_0 + A_1 \ln \dot{\gamma} + A_2 T + A_3(\ln \dot{\gamma})^2 + A_4 T \ln \dot{\gamma} + A_5 T^2 \quad (8)$$

where $A_0, \ldots, A_5$ are constants to be determined. Although this model provides a good fit to the experimental values, it lacks the physical significance of the coefficients of the Eyring model and consequently is unable to describe the structural behavior based on the parameters of the free volume and activation energy of the theoretical model.

The first part of the present study derives the fixed-concentration xanthan gum dispersion flow model from the Ostwald–de Waele model, and the expressions corresponding to consistency and the power law index are obtained as a function of the molar concentration of salt (NaCl) and the temperature. The second part of the study interprets the viscous behavior of the dispersions using the Eyring equation $\eta = f(T)$, and an account is provided of the variation in the parameters of this equation as a function of shear rate and the molar concentration of salt as related to the structure of the dispersions.

EXPERIMENTAL

A total of eight xanthan gum (Burben S.A., Valencia, Spain) dispersions were formulated at a constant concentration of 0.4% (w/w). The NaCl solutions were prepared in distilled water at concentrations of 0, 0.025, 0.050, 0.075, 0.100, 0.150, 0.200, and 0.250M (concentration interval neighboring the most widely used salt concentration[3,4] of 0.1M). A 99.6 g sample was taken from each preparation, 0.4 g of xanthan gum was gradually added to the vortex formed by a magnetic stirrer, and agitation was maintained at approximately 300 rpm for 5 min at room temperature. The preparations were then heated to 80°C and vigorously stirred for 30 min at 1500 rpm using a Heidolph RZR 2021 paddle stirrer. Afterward the formulations were allowed to cool after adding the amount required to restore the initial 100 g of each dispersion following losses to evaporation during the process. Finally, the preparations were stored at room temperature for 24 h, followed by performance of the measurements.

The viscosity determinations of the different dispersions were made using a Bohlin V-88 viscometer. The C30 measurement system was used, corresponding to coaxial cylinders with 30- and 33-mm diameters for the inner and outer cylinders, respectively. Twenty $\dot{\gamma}$ between 30 and 620 s^{-1} were used in approximately logarithmic distribution.

The flow curves $\eta = f(\dot{\gamma})$ were obtained by increasing the $\dot{\gamma}$ every 10 s following a preshear interval of 1 min at the lower rate. For each dispersion the measurements were repeated at six different temperatures in the 20–75°C interval, and the heating and temperature were controlled with a thermostatic bath. It was assumed that the dispersions fully maintain their initial structure in response to stirring, because none of them exhibit thixotropic behavior.

RESULTS AND DISCUSSION

All the flow curves obtained were within the power law region as can be seen from the examples shown in Figures 1 and 2 for 0 and 0.20M saline concentrations and the different temperatures studied.In addition to the shear-thinning behavior,[13] the decrease in the viscosity with temperature is noteable, exhibiting different tendencies in the absence and presence of salt (see below).

The fits to the power model $\eta = K\dot{\gamma}^{n-1}$ ($r > 0.996$) allow us to separately analyze the influences of salt and temperature on the two parameters of the model.

For a given temperature, the power indices ($n - 1$) corresponding to the formulation prepared in

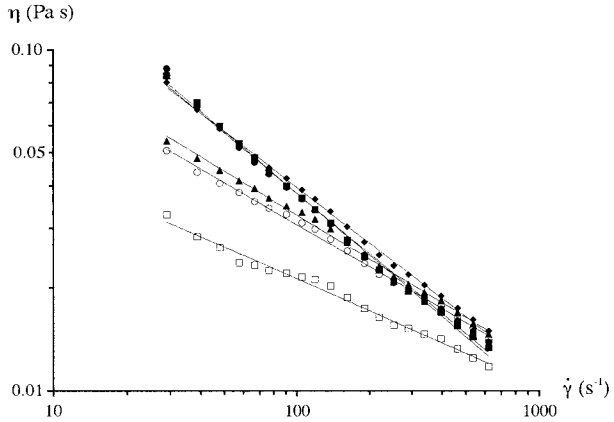

Figure 1 Flow curves of the xanthan gum dispersions prepared in distilled water at (●) 22.5, (■) 32.0, (♦) 40.5, (▲) 53.0, (○) 58.0, and (□) 77.0°C.

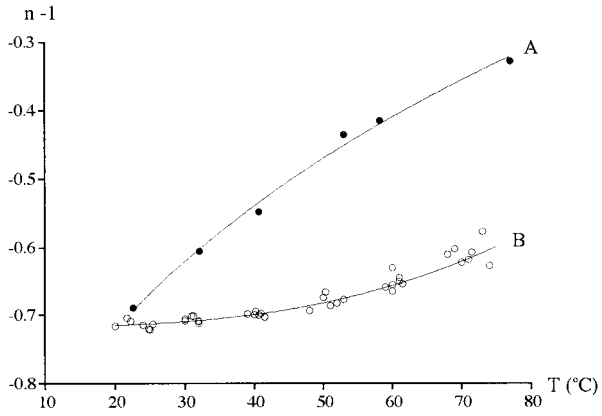

Figure 3 The power law index $(n - 1)$ as a function of temperature for the xanthan gum dispersion without NaCl (curve a) the rest of the dispersions at the different NaCl concentrations studied (curve b).

the absence of NaCl are greater than for the rest of the dispersions. The latter also show that $(n - 1)$ does not undergo significant variations with the NaCl concentration over the range studied.[8] Moreover, the power law index continuously increases (reduction of the shear-thinning character of the dispersions) when the temperature is raised, although in this case the behavior of the dispersion without salt is also different than that of the rest. Figure 3 shows the $(n - 1)$ values obtained as a function of temperature and fitted by potential functions of the following type:

$$(n - 1) = pT^q + s \tag{9}$$

Curve a in Figure 3 corresponds to the xanthan gum dispersion without salt, and curve b corresponds to the rest of the dispersions at the different salt concentrations studied. Thus, two distinct curves were obtained in the absence of salt,

$$(n - 1) = (0.26 \pm 0.01)T^{1/3} - (1.43 \pm 0.04) \qquad r = 0.997 \tag{10}$$

and in the presence of NaCl, regardless of the concentration

$$(n - 1) = (3.00 \pm 0.12)10^{-7}T^3 - (0.718 \pm 0.002) \quad r = 0.970 \tag{11}$$

where $(n - 1)$ is dimensionless and T is the temperature in degrees Celsius. In this latter case an increased variability was observed in the values of $(n - 1)$ corresponding to the highest temperature; this was possibly due to alterations in the sample caused by slight evaporation of the liquid phase.

The comparative analysis of the two equations shows that the shear-thinning rheological behavior of the xanthan gum dispersions is much more sensitive to temperature changes in the absence of NaCl than in its presence, regardless of how small the salt concentration may be and independent of the latter[6] (as previously commented and shown in Fig. 3).

When analyzing the consistency of the dispersions as a function of the molar concentration of NaCl for each of the temperatures studied, the consistency increases on raising the molar concentration of the salt, up to a value of approxi-

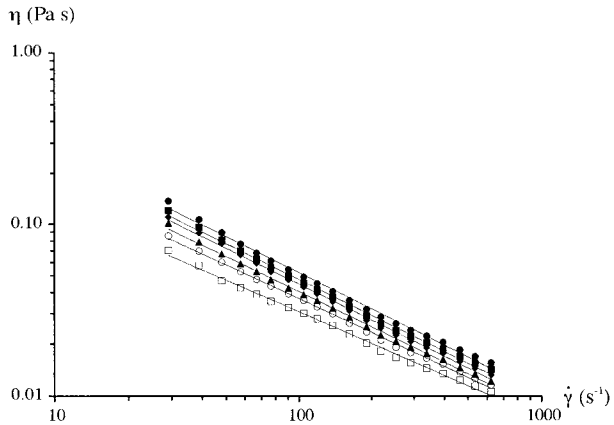

Figure 2 Flow curves of the xanthan gum dispersions prepared in a 0.20*M* NaCl solution at (●) 22.0, (■) 31.0, (♦) 40.0, (▲) 51.0, (○) 60.0, and (□) 71.0°C.

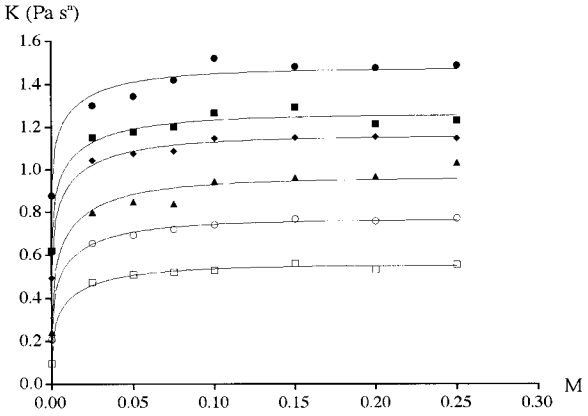

Figure 4 The consistency versus the molar concentration of NaCl at (●) 23.5, (■) 31.0, (♦) 40.5, (▲) 51.0, (○) 60.5, and (□) 71.0°C.

mately 0.1*M*. For higher molar concentration values the *K* tends toward a constant value distinct for each temperature, and that decreases in magnitude as the temperature rises (Fig. 4). Therefore, the distribution of the values $K = f(M)$ corresponding to each temperature must respond to functions with well-defined limiting conditions. Thus, when the molar concentration has very large values ($M \rightarrow \infty$), *K* should tend toward a maximum value (K_{max}) while for $M \rightarrow 0$ the *K* should tend toward a minimum value (K_{min}). Furthermore, the increase in *K* must be very rapid for the lower *M* values and much slower for higher concentrations. One type of function responding to these limiting conditions may be

$$K = K_{min} + (K_{max} - K_{min})(1 - e^{-g(M)}) \quad (12)$$

where $g(M)$ in turn represents as simple a function as possible of the molar concentration of NaCl, which determines the rapidity with which eq. (12) varies. This function should be chosen to allow fitting of the experimental points with sufficiently acceptable correlation coefficients. In the dispersions studied, the following function was selected as a representation of $g(M)$:

$$g(M) = 10M^{1/2} \quad (13)$$

In this way, and based on eqs. (12) and (13), the experimental points represented in Figure 4 were fitted for each of the temperatures studied (continuous lines). The values of K_{max} and K_{min} depend exclusively upon the temperature, because the variation of *K* with the concentration was introduced via eq. (13). Figure 5 shows the values of $K_{max} = f(T)$ and $K_{min} = f(T)$ that were obtained, the fits of which respectively correspond to the equations

$$K_{max} = (1.95 \pm 0.02) - (2.0 \pm 0.1)10^{-2}T \qquad r = 0.994 \quad (14)$$

$$K_{min} = (1.67 \pm 0.02) - (4.1 \pm 0.7)10^{-2}T + (2.5 \pm 0.8)10^{-4}T^2 \qquad r = 0.992 \quad (15)$$

In other words, the maximum value of *K* decreases linearly with the temperature of the dispersion while K_{min} does so in a quadratic manner.

Thus, substitution of expressions (13), (14), and (15) in (12) yields an equation that allows us to determine the consistency of the xanthan gum preparation as a function of temperatures of 20–75°C and NaCl concentrations of 0.000–0.250*M*.

In sum, the results obtained from the study of the xanthan gum dispersions indicate that their rheological behavior corresponds to that of a shear-thinning fluid that responds well to the power law over the shear rate interval employed. The power law index is much less sensitive to changes in temperature when NaCl is added even in very small amounts. However, a temperature rise reduces the shear-thinning characteristics of the system as reflected by the resulting increase in the power law index ($n - 1$). In regard to the consistency of the dispersions, it was shown that the lowest *K* values correspond to the dispersions formulated in the absence of salt and the highest are for molar values ≥0.15, and there are de-

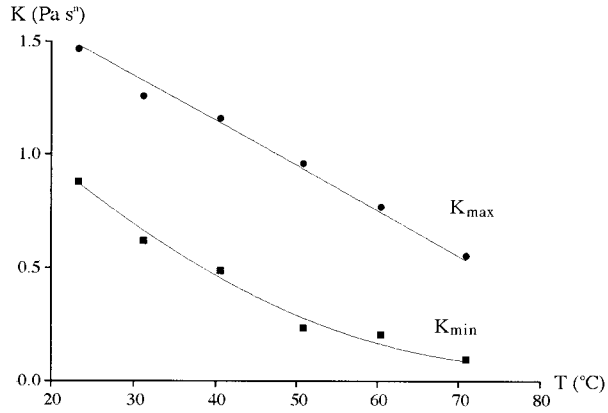

Figure 5 The maximum and minimum values of consistency as a function of the temperature.

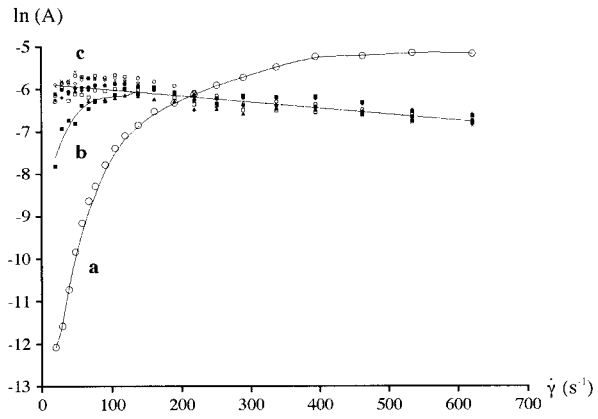

Figure 6 Parameter A in the Eyring equation as a function of the shear rate for the xanthan gum dispersions at NaCl concentrations of 0 (curve a) and 0.025M (curve b) and the rest of the concentrations (>0.025M, curve c).

creases in K when the temperature is raised in all cases.

Although the xanthan gum dispersions evaluated in the present work cannot be strictly regarded as pure fluids, the dependency of their viscosity on the temperature allowed their study based on the theory of fluid kinetics developed by Eyring. To this effect and based on the experimental measurements $\eta = f(\dot{\gamma}, M, T)$, the values of $\eta = f(T)$ were fitted, where T is the thermodynamic temperature (K) for each molar concentration and shear rate, by means of equations of the following type:

$$\ln \eta = \ln A + \frac{B}{RT} \qquad (16)$$

where B represents the activation energy . In this way we obtained a total of 160 equations (20 for each molar concentration), and over 95% exhibited correlation coefficients above 0.990.

Figure 6 shows the ln A values obtained as a function of the shear rate for each of the NaCl concentrations. It can be seen in curve a in Figure 6 (corresponding to the xanthan gum formulation without salt) that the ln A increases in a constant manner when raising the shear rate. Because parameter A is inversely proportional to the free volume , this means that the latter decreases very rapidly on increasing the $\dot{\gamma}$. This fact can be explained by supposing that, at rest, the polymer molecules form coils and leave large portions of water between them toward which displacement is possible. The increase in $\dot{\gamma}$ favors rupture and separation of these coils, leading to homogenization of the dispersion and therefore to a diminished free volume. This explains the tendency of A toward a constant value beyond shear rates of about 350–400 s^{-1}, because at high rates all the purported polymer packing was disrupted.

In all the other dispersions formulated with NaCl, the ln A was practically independent of the salt concentration and slightly decreased when the shear rate was elevated (Fig. 6 curve c). The least squares linear fit of $A = f(\dot{\gamma})$ yields the expression

$$A = (2.66 \pm 0.06)10^{-3} - (2.4 \pm 0.2)10^{-6}\dot{\gamma} \qquad r = 0.991 \quad (17)$$

where A is given in Pascal seconds (Pa s) and $\dot{\gamma}$ is per second (s^{-1}). Deviation from the general behavior is only observed for the ln A values corresponding to a concentration of 0.025M (graph b), which are found between the concentrations of 0 and >0.025M for the lowest shear rates of <70 s^{-1}.

This behavior of parameter A can be accounted for by the effect of adding electrolytes to the xanthan gum molecules with the arrangement of the chains[9] and their posterior dissociation, which would yield a 3-dimensional network capable of trapping water and thus a decrease in the free volume of the dispersion. However, the increase in the shear rate is able to disrupt the weak bonds between the coil structures forming the network with the subsequent release of the trapped water and a resulting growth in the free volume of the formulation. This interpretation would explain the higher A values at low $\dot{\gamma}$ and the slight decrease of A on increasing $\dot{\gamma}$, as observed in Figure 6 (curve c). In fact, from eq. (17) we ascertain that the highest value of A for the lowest shear rate considered (29 s^{-1}) is $A_{max} = 2.6 \times 10^{-3}$ Pa s, while for 620 s^{-1} it is $A \approx 1.5 \times 10^{-3}$ Pa s. Taking eq. (3) into account, that implies a 1.7-fold increase in the free volume, which was produced by the increase in the shear rate.

The equality (within the margins of error) of the A values at a given shear rate for the xanthan gum dispersions formulated with NaCl concentrations above 0.025M indicates that the effect of adding electrolytes upon the molecular structure of xanthan gum is independent of the NaCl concentration within the range analyzed in this study.

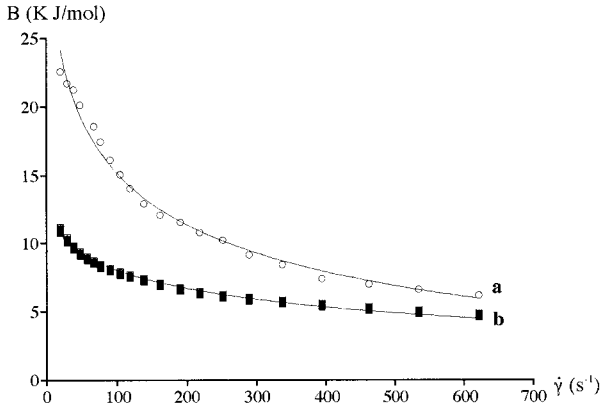

Figure 7 Parameter B in the Eyring equation as a function of the shear rate for the xanthan gum dispersions without NaCl (curve a) and the NaCl concentrations (curve b).

In addition, comparison of curves a and c in Figure 6 show that for values of $\dot{\gamma} > 250$ s^{-1}, the free volume of the dispersion formulated with salt is greater than for the preparations without salt. This can be explained by both the network disruption at high shear rates and the posterior autoassociation of the xanthan gum molecules due to the presence of the electrolytes.[8]

On the other hand, the activation energies ($B = G^{+}$) were likewise calculated from the fits made with eq. (16), taking into account that $R = 8.314 \times 10^{-3}$ kJ mol^{-1} K^{-1}. Figure 7 shows the values of B obtained as a function of the shear rate for the xanthan gum formulations without NaCl and for all the other preparations. Attention is drawn to the important effect of the NaCl addition, which reduces the activation energy, regardless of the salt concentration. As would be expected considering eq. (1), the activation energy decreases progressively in all cases when $\dot{\gamma}$ is raised, because an increase in the shear rate implies an increased shear stress in this type of dispersion with shear-thinning characteristics (Fig. 7). The values of B (kJ mol^{-1}) were fitted by means of expressions of the following kind:

$$G^{+} = B = K_1 \exp(-K_2 \dot{\gamma}^m) \quad (18)$$

where K_2 and m are two positive coefficients and K_1 represents the activation energy, corresponding to $\dot{\gamma} = 0$. The equations obtained (graphically represented as continuous lines in Fig. 7) are

$$B = (46.2 \pm 1.5)\exp[-(0.240 \pm 0.007)\dot{\gamma}^{1/3}] \quad r = 0.994 \quad (19)$$

for the dispersion in the absence of salt and

$$B = (15.9 \pm 0.3)\exp[-(0.148 \pm 0.003)\dot{\gamma}^{1/3}] \quad r = 0.997 \quad (20)$$

for the rest of the formulations with NaCl, regardless of the molar concentration involved. If we accept the extrapolation of these functions for a shear rate of zero, then activation energies of 46.2 $\pm$ 1.5 and 15.9 $\pm$ 0.3 kJ mol^{-1} would be obtained. In other words, the activation energy obtained at $\dot{\gamma} = 0$ is about 3 times greater in the absence of salt than in its presence. The value obtained for the activation energy at low shear rates in saline dispersions and the fact that it is independent of the salt concentration both agree with the results obtained by Launay et al.[14] On the other hand and for most shear rates studied, the formulations without salt presented activation energies only about 1.3 times greater than those of the rest of the dispersions investigated. Logically, when incrementing the shear rate, the B values for both types of dispersion (with and without NaCl) tend to equalize, as was seen in the A values. This, in sum, would explain why the viscosities of all the formulations tend to be practically identical as was demonstrated experimentally and depend almost exclusively on the temperature.

These results are consistent with the explanation given for the molecular arrangement of xanthan gum, which was deduced by analyzing the values of A. In effect, in the dispersion without NaCl the transfer of the xanthan gum molecular coils from one space or gap to another requires more energy than that needed to transfer ordered molecules like those that form in the presence of electrolytes. In other words, despite the greater number of gaps present in the dispersions without salt, at lower shear rates the molecular displacement from one gap to another requires greater activation energy because of the need to transfer molecular conglomerates.

REFERENCES

1. Zatz, J. L.; Knapp, S. J Pharm Sci 1984, 73, 468.
2. Ferguson, J.; Kemblowski, Z. Applied Fluid Rheology; Elsevier: Amsterdam, 1991; Chapters 4, 5, and 7.
3. Kang, K. S.; Pettitt, D. J. In Industrial Gums. Polysaccharides and Their Derivatives; Whistler, R. L., BeMiller, J. N., Eds.; Academic: London, 1993; Chapter 13.

4. Lapasin, R.; Pricl, S. Rheology of Industrial Polysaccharides: Theory and Applications; Blackie Academic & Professional: Glasgow, Scotland, 1995; Chapters 2 and 4.
5. Nussinovitch, A. Hydrocolloid Applications; Blackie Academic & Professional: London, 1997; Chapter 9.
6. Chinnaswamy, R.; Hanna, M. A. Indian Food Ind 1993, 12, 27.
7. Technical information from Jungbunzlauer, presented at AFCA Congress, Barcelona, 1996.
8. Pastor, M. V.; Costell, E.; Izquierdo, L.; Durán, L. Food Hydrocolloid 1994, 8, 265.
9. Williams, P. A.; Day, D. H.; Langdon, M. J.; Phillips, G. O.; Nishinari, K. Food Hydrocolloid 1991, 4, 489.
10. Xiong, Y. L.; Noel, D. C.; Moody, W. G. J Food Sci 1999, 64, 550.
11. Hernández, M. J.; Hudson, N. In Proceedings of the XIIIth International Congress on Rheology; Binding, D. M. et al., Eds.; British Society of Rheology: Glasgow, Scotland, 2000; Vol. 4, p 414.
12. Ma, L.; Barbosa-Cáovas, G. V. J Food Sci 1997, 62, 1124.
13. Milas, M.; Rinaudo, M. Carbohydr Res 1979, 76, 189.
14. Launay, B.; Cuvelier, G.; Martínez-Reyes, S. Carbohydr Polym 1997, 34, 385.
15. Bird, R. B.; Stewart, W. E.; Loghtfoot, E. N. Transport Phenomena; Wiley: New York, 1960; Chapter 1.
16. van Wazer, J. R.; Lyons, J. W.; Kim, K. Y.; Colwell, R. E. Viscosity and Flow Measurement. A Laboratory Handbook of Rheology; Interscience Publishers: New York, 1963; Chapter 1.
17. Yang, M. C.; Perng, J. S. J Appl Polym Sci 2000, 76, 2068.
18. Tanner, R. I. Engineering Rheology, 2nd ed.; Oxford University Press: New York, 2000; Chapter 9.
19. Kennedy, P. Flow Analysis of Injection Molds; Hanser: Munich, 1995.